

Fast Prototyping for Atmospheric Plasma Sources Integration into Air Hand Dryers

Abdel Majid Kassir, Joël Sonnard, Ludovic Roulin, Martine Baudin, Gilles Courret, Wolfram Manuel Brück

Abstract—Motivated by the current COVID-19 pandemic and the need to find alternative methods to contain and battle it, the purpose of this innovative project is to conceive a disinfection module equipped with a cold atmospheric plasma source. Such a plasma source was developed for a potential integration into pulsed air hand dryers. This type of plasma is known for its ability to generate reactive oxygen and nitrogen species that initiate bio-molecular reactions involved in bacterial and viral deactivation mechanisms. This study shows how additive manufacturing helped accelerate the prototyping of a nozzle allowing the preservation of the plasma flow from circulation cells and external interferences in the discharge’s surrounding.

Keywords—Cold atmospheric plasma, hand disinfection, hand sanitization, bacterial and viral deactivation, plasma chemistry.

I. INTRODUCTION

MOST countries were and still are strongly affected by the current COVID-19 pandemic. Despite many lockdowns restricting people’s movement and interactions, the virus spread across the planet. The means of combating this highly contagious disease consist mainly of sanitary measures where hand hygiene is crucial. Consequently, hydro-alcoholic gels were highly sought after following a global consensus recommending their use for hand disinfection. In the context of this pandemic, pulsed air hand dryers are suspected to be potential sources of virus dissemination due to aerosols carried by circulatory cells [1]. The purpose of this research project was to develop a rapid prototyping technique for disinfection modules equipped with a cold atmospheric plasma (CAP) source capable of preventing the risk of contamination in air hand dryers. Unlike thermal plasmas, cold plasmas are characterized by a high electronic temperature while the gas temperature, which characterizes the energy of heavy particles, is only slightly higher than the ambient temperature [2, p.21]. The exposed surface or living tissue can therefore be protected from damage or injury. Many applications of CAPs have been found in the last decade, in biomedicine, nanomaterials, agriculture, and water purification [3]. It is known that Reactive Oxygen and Nitrogen Species (RONS) generated in such plasmas make a significant contribution into sterilization [4, p.855]. From a technical point of view, our intention was to reduce the prototyping time of a nozzle adapted to the hand dryers’ aerualics.

This study is a collaborative work between the Institute of Life Technologies (ITV) of the HES-SO Valais-Wallis, where the bacterial cultivation of *Escherichia coli* (DSM682) and

Staphylococcus epidermidis (DSM20044) and the analysis of the microbiological tests were carried out, and the Institute of Energy and Electrical Systems (IESE) of the HEIG-VD where the prototyping of the plasma set-ups and the drive assemblies were conducted. The samples prepared at the ITV were exposed and treated in a controlled manner using the plasma sources developed at the IESE.

A direct current (DC) atmospheric cold plasma was conceived in two configurations regarding the grounding and the plasma flow control using a nozzle. The light emitted by the plasma was collected by an optical fiber and sent to the entrance slit of a spectrometer allowing the visualization of the optical emission spectrum of the discharge. The plasma temperature was monitored with a FISO FTI-10 thermometer. Finally, the surface temperature of the Petri dish and the metallic plates was monitored using a FLIR A8580 IR camera.

II. PLASMA SOURCE WITH A GROUNDED GRID FOR INDIRECT TREATMENT

A. Design

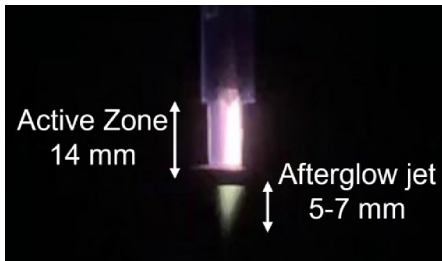
The DC plasma source was inspired by [5]. The discharge was generated in a pin-to-mesh electrodes configuration inside a fused silica tube of 5 mm of inner diameter. The cathode consisted of a conically sharpened 3.2 mm diameter tungsten rod placed at the center of the tube and connected to the negative polarity of a DC high-voltage (HV) power supply through a ballast resistor of 880 kΩ. A grounded stainless steel fine mesh metallic grid of 0.596 mm aperture was placed at the tube’s outlet and acted as an anode. The ballast resistor prevents the glow-to-arc transition and ensures that the discharge operates in a stable regime. To enhance the production of RONS, dry air was used as a plasma gas and was injected inside the tube via a 5 mm inlet, and the flow was monitored using a flow sensor. The operational conditions are summarized in Table I.

When the HV is applied between the electrodes and the breakdown occurs, two distinctive plasma regions can be visually identified: (1) the active zone (AZ) located between the pin and the mesh and (2) the afterglow (AG) downstream from the mesh (cf. Fig. 1 (a)). An optical fiber thermometer (FISO FTI-10) was placed 5 mm away from the tube outlet and was used to measure the AG jet temperature. Finally, a railing comprised of a linear drive and a rotary motor complete this configuration allowing the exposure of a Petri dish to the AG jet in a controlled manner.

Gilles Courret is with School of Engineering and Management Vaud (HEIG-VD), Switzerland (e-mail: gilles.courret@heig-vd.ch).

TABLE I
 OPERATIONAL CONDITIONS OF THE DC CONFIGURATIONS

Configuration	Voltage kV	Ballast $k\Omega$	Current mA	Electrode spacing mm	Air flow l/min
Indirect treatment	12 - 20	880	13 - 22	14	12 - 16
Direct treatment	12 - 20	880	13 - 22	14	28 - 32



Photograph of the DC discharge showing the active zone (AZ) and the afterglow (AG).

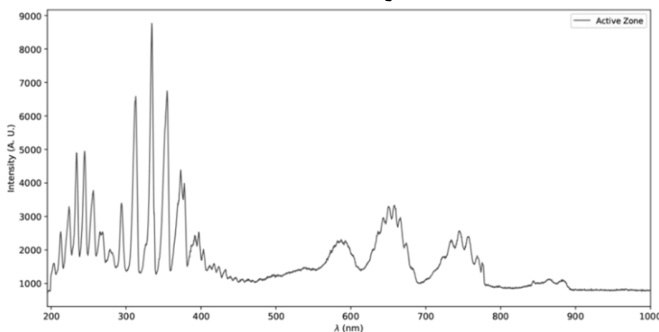


Fig. 1 (a) Photograph of the DC discharge, (b) Optical emission spectrum of a dry air plasma in the active zone

Optical diagnostics of the discharge was carried out by means of Optical Emission Spectroscopy, the most classical and non-intrusive technique, allowing (1) the identification of light-emitting species within the plasma with minimal equipment and (2) the estimation of the rotational and vibrational temperature of the molecules if the spectrum is sufficiently resolved. The measured emission spectrum of the dry air plasma in the AZ spanning the spectral range of 200–1000 nm is shown in Fig. 1 (b). This spectrum can be decomposed as follows, according to the chemical composition:

 TABLE II
 ANALYSIS OF THE OPTICAL EMISSION SPECTRUM SHOWN IN FIG. 1 (B)

Spectral range nm	Emitting species
200 - 300	NO electronic system with a possible interference from the NO ϵ and δ systems as well as the O_2 Schumann-Runge system (unresolved on Fig. 1).
300 - 380	N_2 Second Positive System with a possible interference between 306 and 310 nm originating from the OH Violet system.
380 - 480	N_2^+ First Negative System
480 - 900	N_2 First Positive System

B. Microbiological Tests

To test the disinfection power of the DC plasma source, described in Section II A, a series of qualitative preliminary

trials was conducted on test samples of the bacteria (*E. coli* and *S. epidermidis*) dried on metallic plates and cultivated in Petri dishes. The plasma temperature in the AG jet was controlled before the trials and found to be in the vicinity of 60 °C at the tip of the AG jet. Albeit the jet's temperature being higher than the biological tolerance temperature of 37 to 40 °C, the trials occurred in hand-drying operational conditions—exposure distance of 4.5 cm and exposure time of 15 s. In these conditions, the temperature of the plasma jet dropped to 30–35 °C, thus preventing a thermal overload on the samples. Finally, the procedure consisted of (1) placing the Petri dish containing THE BACTERIA OR THE METALLIC PLATE IN THE DEDICATED PLACE ON TOP of the rotary motor at 4.5 cm away from the jet and 4 RPM, and (2) perform back-and-forth sweeps under the plasma jet using the linear drive.

The results of disinfection are shown in Figure 2 (A). Upon comparing the dishes of the top row with those of the bottom row, it can be deduced that no disinfection effect was observed following the plasma treatment: the growth of the bacteria continued its course. The absence of disinfection was attributed to the lack of chemical reactivity of the plasma in the AG jet. Indeed, upon examining the jet's emission spectrum, presented in Figure 2 (B), this explanation seems satisfactory. It's straightforward to see that the molecular emission of N_2 , N_2^+ , and NO dropped significantly in the AG jet compared to the AZ in Figure 1 (B), and some line signatures of atomic oxygen and nitrogen are detected due to the possible dissociation of N_2 and O_2 from ambient air mixed into the jet by circulation cells. It is thus believed that the metallic mesh—acting as an anode—freezes the chemistry by trapping electrons and charged radicals thus hindering the formation of complex compounds such as peroxides in the AG jet [6]. To preserve the plasma flow from external intruders that can deplete the chemical reactivity of the plasma, on which the disinfection performance depends, a new prototype configuration equipped with a nozzle was developed and is described in the following section.

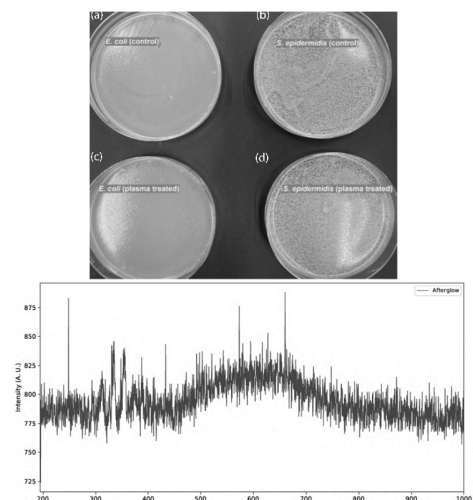


Figure 2 : A. Control Petri dishes (a)&(b) and plasma treated bacteria (c)&(d). B. Optical Emission Spectrum of the dry air plasma in the afterglow jet.

3/ Plasma source without a grounded grid for direct treatment

3.1/ Configuration

Following these inadequate results, the DC plasma source was modified to allow for a direct treatment of the contaminated surface. In this configuration, the treated surface is part of the electrical circuit of the discharge: it can be grounded or have a high capacity for charge storage, known as a floating electrode configuration, introduced by Fridman et al. in 2006 [7]. Moreover, the degree of freedom offered by the two motors was deemed insufficient and was replaced by a 3-axis scanning system controlled by an Arduino board and offering micrometric precision in terms of exposure distance tuning as well as user-defined scanning profiles to fit the geometry of the treated object. This atmospheric DC plasma source is shown in Figure 3. The operating conditions were kept the same except for the air flow which was increased in this configuration (cf. Table 1).

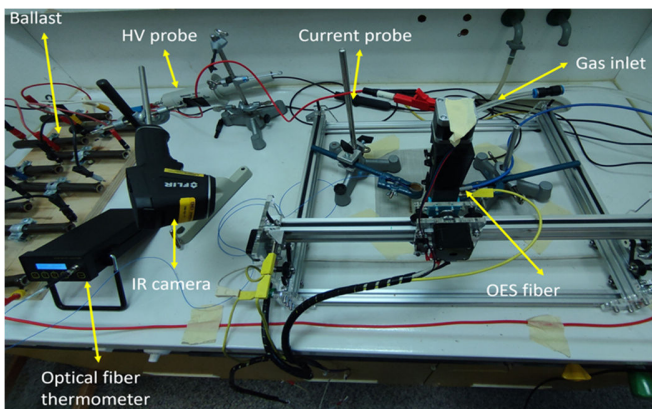


Figure 3 Photograph of the modified DC plasma source and scanning system.

3.2/ Microbiological test

The disinfection capabilities of this new configuration were tested during a second series of microbiological tests carried out on metallic plates directly connected to the ground, using an assay adapted from Sen and Mutlu [8]. This setup allowed the plasma's active zone to extend from the tungsten rod's tip to the surface of the plate on which the bacteria were cultivated as can be seen in Figure 4 (A). Before conducting the second series of tests, the optical emission spectrum of the discharge was collected near the plate's surface and is plotted in

Figure 4 (B).

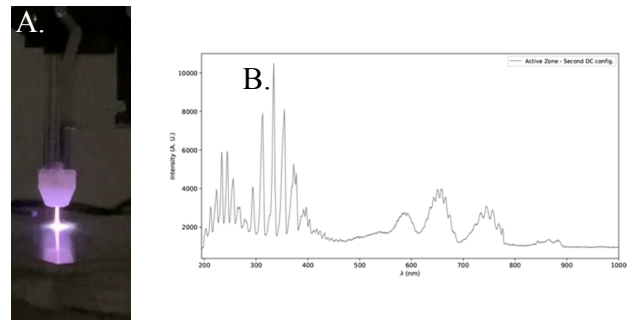


Figure 4: A. Photograph of the discharge in the modified version of the DC source. B. Optical emission spectrum of the dry air plasma in the active zone.

It can be easily inferred that the spectrum of Figure 4 (B) shows the exact same structures seen on the spectrum of Figure 1 (B) which confirms that the metallic grid was indeed inhibiting the development of the complex chemistry necessary to induce the bacterial inactivation. The discharge's temperature was monitored by the optical fiber thermometer and found to be in the vicinity of 30 °C. The plasma was maintained at this temperature during the tests described below by a high dry air flow of 28 to 32 l/min [5].

3.3/ Fast nozzle prototyping

To avoid the appearance of circulation cells due to the high flows used in the gridless configuration, a nozzle of 3.5 mm diameter was inserted at the tube outlet, which is presented in Figure 5. Adapting the plasma jet's aerodynamics for optimal integration in an air hand dryer requires testing many nozzle designs and sizes. A significant time saving is achieved by avoiding the redesigning of the entire quartz tube and by conceiving the nozzle using additive manufacturing (3D printing). The manufacturing time of a glass tube prototype is of the order of a few weeks due to the required specific skills in glass blowing. In contrast, the manufacturing time of a 3D printed nozzle, here with a translucent bio-based engineering plastic branded Durabio, is of the order of a few hours. This material being organic, the temperature of the plasma flow must however be constantly monitored and controlled.

Nozzles with diameters between 2.5 and 4.5 mm were tested. Starting with the smaller, the nozzle visibly prevented the plasma jet from fully propagating into ambient air, which led to a slow

decay of the nozzle's interior walls, ending with its complete deformation. As for the 4.5 mm nozzle, two small-scale lateral plasma jets were observed, in addition to the central jet. These lateral jets interacted with the nozzle's exterior walls and slowly deformed the outlet's shape and diameter. The appearance of the additional jets could be assigned to the formation of circulation cells in the surroundings of the nozzle's outlet. Finally, the 3.5 mm was deemed to be the most appropriate for the current configuration, especially after estimating a plasma jet diameter of 3 to 3.2 mm. It is believed that with the 3.5 mm nozzle, a cold air sheath is created around the jet, keeping it from interacting with the nozzle's walls. For 3D printing purposes, the nozzle's sharp edges were smoothed out using the fillet feature in Solidworks®, as demonstrated in Figure 5.

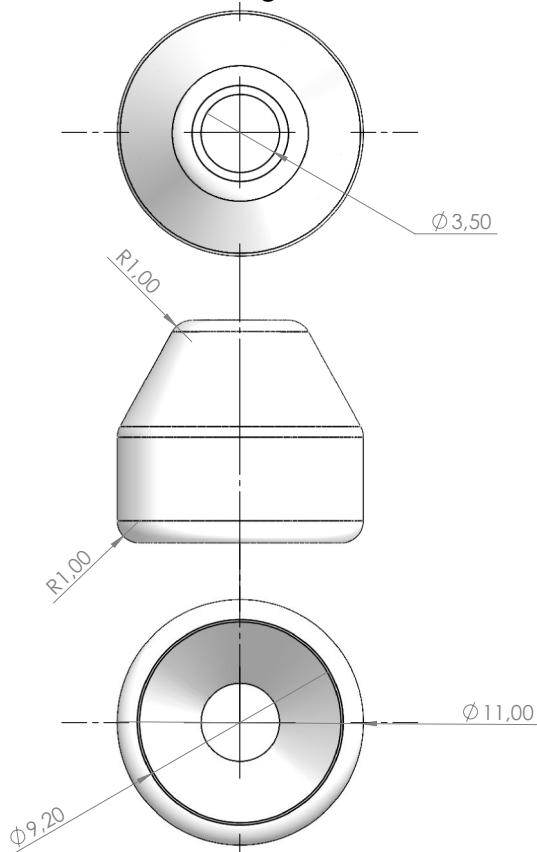


Figure 5: CAD drawing of the nozzle

Hence, this nozzle plays a dual role: (1) it prevents the mixing of ambient air into the discharge near the tube outlet, which can impoverish the plasma in active species by recombination processes, and (2) it channels the plasma jet into a straight column with an impact radius of 4.5 mm, estimated by drawing circles of various diameters on a test plate.

3.4/ Microbiological test

Encouraged by the outcome of this modified version of the DC source in terms of emission spectrum, jet temperature, and scanning freedom, another campaign of qualitative disinfection tests was conducted on samples of bacteria dried on sterile 5 x 5 cm metallic plates. A set of four plates was tested for each type of bacteria with scanning times ranging from 30 to 120 s with an increment of 30 s. These scanning times correspond to the duration necessary to scan the 25 cm² area of the plate, starting at 4 cm/s for a 30 s scanning time and ending at 1 cm/s for 120 s. The qualitative results of these tests are presented in Figure 6.

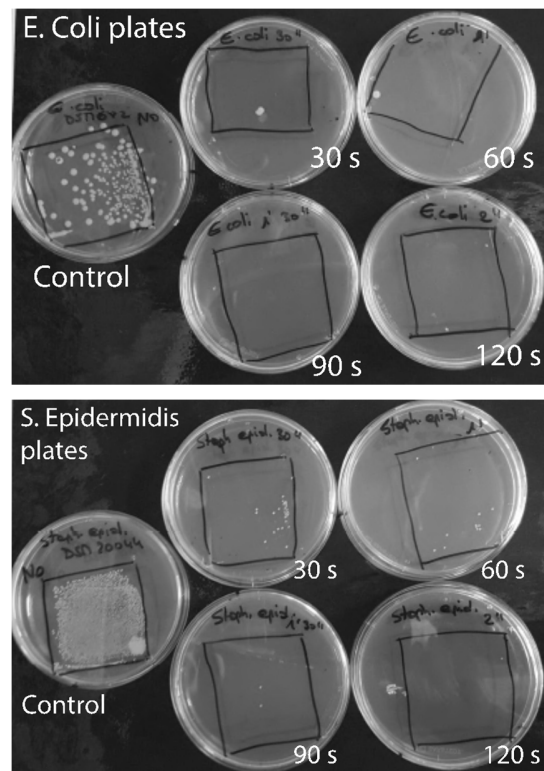


Figure 6: A. Disinfection of *E. Coli*-contaminated plates. B. Disinfection of *S. Epidermidis*-contaminated plates.

A close examination of Figure 6 shows the clear and visible effect of the plasma treatment of the plates even for a duration as short as 30 seconds and an almost complete bacterial inactivation after 120 seconds. Following this qualitative trial, a quantitative assay was planned. Known dilutions of the two microorganisms used previously were applied to metallic chips of 2 cm diameter. The chips were dried and placed on a grounded 5 x 5 cm plate. A total of three sets of four chips—two per bacterial

type—was prepared for this campaign and to each set corresponded a scanning time, namely 30 s, 60 s, and 120 s. These times correlate with the duration necessary to scan the 25 cm² area of the plate, i.e. the plate was entirely and uniformly exposed to the plasma jet during the three time intervals mentioned above. Therefore, the 30 s corresponded to a scan rate of 4 cm/s, the 60 s to 2 cm/s, and the 120 s to 1 cm/s. Following the treatment, the chips were separated and submerged in a physiological saline solution and transported to the ITV for quantitative analysis. The results are documented in the Tables 2 and 3 for the *E. coli* (DSM682) and the *S. epidermidis* (DSM 20044), respectively.

These results show that the longest scanning time yielded the better log reduction of approximately 2 (cf. bottom rows). This can be understood in terms of interaction time between the plasma jet and the chips. Indeed, the 120 s scanning time corresponds to the slowest scanning rate of 1 cm/s offering the longest contact between the chips' surface and the plasma flow transporting the reactive species (cf. Figure 4). The log reduction factors obtained here are coherent and comparable to those found in the literature on a similar plasma configuration [6].

Tableau 3 Results of the *E. coli* (DSM682) load reduction using the modified DC source, with grounded samples.

Non-treated control chip a	Non-treated control chip b	Treated chip 30 s a	Treated chip 30 s b	Treated chip 60 s a	Treated chip 60 s b	Treated chip 120 s a	Treated chip 120 s b
6.2 10 ⁶	5.1 10 ⁶	2.2 10 ⁵	1.4 10 ⁵	5.6 10 ⁴	5.7 10 ⁴	8.1 10 ³	4.2 10 ³
log 5.79	log 5.71	log 5.34	log 5.15	log 4.75	log 4.76	log 3.91	log 3.62
log 5.75		log 5.24		log 4.75		log 3.77	
Log reduction		0.51		1.00		1.98	

Tableau 4 Results of the *S. epidermidis* (DSM20044) load reduction using the modified DC source, with grounded samples.

Non-treated control chip a	Non-treated control chip b	Treated chip 30 s a	Treated chip 30 s b	Treated chip 60 s a	Treated chip 60 s b	Treated chip 120 s a	Treated chip 120 s b
2.1 10 ⁶	2.1 10 ⁶	6.8 10 ⁵	5.8 10 ⁵	3.1 10 ⁵	1.7 10 ⁵	3.7 10 ⁴	2.9 10 ⁴
log 6.32	log 6.32	log 5.83	log 5.76	log 5.49	log 5.24	log 4.57	log 4.45
log 6.32		log 5.80		log 5.37		log 4.51	
Log reduction		0.52		0.96		1.81	

3/ Conclusion

Two DC plasma sources were developed in two different grounding configurations:

- with a grounded grid
- without a grid but a grounded targeted surface.

The second configuration is only applicable to

electrically conductive materials. The tests confirmed that the direct treatment of contaminated surfaces following the removal of the grounded grid yield a clear and efficient disinfection process. Aided by the optical emission spectra, the absence of disinfection effect in the first configuration was attributed to the lack of chemical reactivity of the plasma in the AG jet. It is thus believed that the metallic mesh freezes the chemistry by trapping electrons and charged radicals thus hindering the formation of the disinfecting compounds in the AG jet.

The integration in air hand dryers of a plasma module of the second configuration type could well reduce the risk of contamination due to aerosols spreading the virus in the air. In addition to the direct disinfection effect of the CAP, the jet could indeed charge the aerosols so that they are drained towards the grounded surface where they will then be neutralized, comparable to an electrostatic filter, a technique used to remove viruses from gases [9]. Adapting hand dryer nozzles to this application would be greatly accelerated with 3D additive printing.

4/ Bibliography

[1] Recommandations relatives à la ventilation des bâtiments hors hôpital et institutions de soin pour limiter la transmission de SARS-COV-2 par voie aéroportée, Conseil Supérieur de la Santé, Bruxelles, CSS n°9616, février 2021.

[2] K H Becker, U Kogelschatz, K H Schoenbach, R J Barker, Non-equilibrium Air Plasmas at Atmospheric Pressure, IOP Publishing Ltd, 2005

[3] Li Lin, Michael Keidar, A map of control for cold atmospheric plasma jets, Appl. Phys. Rev. 8, 011306 (2021)

[4] Alexander Fridman, Plasma Chemistry, Cambridge University Press, 2008

[5] XL Deng, A Yu Nikiforov, Patrick Vanraes, and Ch Leys, Direct current plasma jet at atmospheric pressure operating in nitrogen and air, Journal of Applied Physics, 113(2):023305, 2013.

[6] Danil Dobrynin, Gary Friedman, Alexander Fridman, and Andrey Starikovskiy, Inactivation of bacteria using dc corona discharge: role of ions and humidity, *New journal of physics*, 13(10):103033, 2011.

[7] Gregory Fridman, Marie Peddinghaus, Manjula Balasubramanian, Halim Ayan, Alexander Fridman, Alexander Gutsol, and Ari Brooks, Blood coagulation and living tissue sterilization by floating-electrode dielectric barrier discharge in air, *Plasma Chemistry and plasma processing*, 26(4):425–442, 2006.

[8] Yasin Sen and Mehmet Mutlu, Sterilization of Food Contacting Surfaces via Non-Thermal Plasma Treatment: A Model Study with *Escherichia coli*-Contaminated Stainless Steel and Polyethylene Surfaces, *Food and Bioprocess Technology*, 6: 3295–3304, 2013. <https://doi.org/10.1007/s11947-012-1007-2>.

[9] Dee, S. A., Deen, J., Cano, J. P., Batista, L., & Pijoan, C. Further evaluation of alternative air-filtration systems for reducing the transmission of porcine reproductive and respiratory syndrome virus by aerosol, *Canadian Journal of Veterinary Research*, 70(3), 168, 2006.